Immunoglobulin Class Switch Recombination Is Impaired in *Atm*-deficient Mice

Joanne M. Lumsden,[1] Thomas McCarty,[2] Lisa K. Petiniot,[1,3] Rhuna Shen,[1,3] Carrolee Barlow,[4] Thomas A. Wynn,[5] Herbert C. Morse III,[2] Patricia J. Gearhart,[8] Anthony Wynshaw-Boris,[4] Edward E. Max,[6] and Richard J. Hodes[1,7]

[1]*Experimental Immunology Branch, National Cancer Institute,* [2]*Laboratory of Immunopathology, National Institute of Allergy and Infectious Diseases (NIAID),* [3]*Howard Hughes Medical Institute - National Institutes of Health Research Scholars Program,* [4]*Genetic Disease Research Branch, National Center for Human Genome Research,* [5]*Laboratory of Parasitic Diseases, NIAID,* [6]*Center for Drugs Evaluation and Research, Food and Drug Administration, and* [7]*National Institute on Aging, National Institutes of Health (NIH), Bethesda, MD 20892*
[8]*Laboratory of Molecular Gerontology, National Institute on Aging, NIH, Baltimore, MD 21224*

The Journal of Experimental Medicine

Abstract

Immunoglobulin class switch recombination (Ig CSR) involves DNA double strand breaks (DSBs) at recombining switch regions and repair of these breaks by nonhomologous end-joining. Because the protein kinase ataxia telengiectasia (AT) mutated (ATM) plays a critical role in DSB repair and AT patients show abnormalities of Ig isotype expression, we assessed the role of ATM in CSR by examining ATM-deficient mice. In response to T cell–dependent antigen (Ag), $Atm^{-/-}$ mice secreted substantially less Ag-specific IgA, IgG1, IgG2b, and IgG3, and less total IgE than $Atm^{+/+}$ controls. To determine whether $Atm^{-/-}$ B cells have an intrinsic defect in their ability to undergo CSR, we analyzed in vitro responses of purified B cells. $Atm^{-/-}$ cells secreted substantially less IgA, IgG1, IgG2a, IgG3, and IgE than wild-type (WT) controls in response to stimulation with lipopolysaccharide, CD40 ligand, or anti-IgD plus appropriate cytokines. Molecular analysis of in vitro responses indicated that WT and $Atm^{-/-}$ B cells produced equivalent amounts of germline IgG1 and IgE transcripts, whereas $Atm^{-/-}$ B cells produced markedly reduced productive IgG1 and IgE transcripts. The reduction in isotype switching by $Atm^{-/-}$ B cells occurs at the level of genomic DNA recombination as measured by digestion–circularization PCR. Analysis of sequences at CSR sites indicated that there is greater microhomology at the μ–γ1 switch junctions in ATM B cells than in wild-type B cells, suggesting that ATM function affects the need or preference for sequence homology in the CSR process. These findings suggest a role of ATM in DNA DSB recognition and/or repair during CSR.

Key words: ataxia telangiectasia • Ig class switching • B lymphocytes • DNA damage • DNA repair

Introduction

The production of Ig isotypes other than IgM and IgD is accomplished by a deletional recombination event that brings a downstream C_H gene into proximity with V(D)J elements, resulting in generation of antibodies of different isotypes and effector function, but with unaltered antigen (Ag) specificity. In this process of class switch recombination (CSR), intrachromosomal recombination occurs between tandemly repeated switch (S) region sequences located upstream of each Ig heavy chain constant region gene, with

J.M. Lumsden, T. McCarty, L.K. Petiniot, and R. Shen contributed equally to this work.

Address correspondence to Joanne Lumsden, Experimental Immunology Branch, National Cancer Institute, National Institutes of Health, Bldg. 10, Room 4B10, 10 Center Dr., Bethesda, MD 20892. Phone: (301) 435-6462; Fax: (301) 496-0887; email: lumsdenj@mail.nih.gov

The present address of C. Barlow is Merck Research Laboratories, San Diego, CA 92121.

The present address of A. Wynshaw-Boris is UCSD School of Medicine, La Jolla, CA 92093.

Abbreviations used in this paper: Ag, antigen; AID, activation-induced cytidine deaminase; AT, ataxia telangiectasia; ATM, ataxia telangiectasia mutated; CD40L, CD40 ligand; CSR, class switch recombination; DC-PCR, digestion-circularization PCR; nAChR, nicotinic acetylcholine receptor; NHEJ, nonhomologous end-joining; PNA, peanut agglutinin; S, switch; TD, T cell–dependent.

excision of intervening sequences in the form of circular DNA.

CSR involves the induction of DNA breaks in Sμ and a downstream target S region, followed by ligation through a nonhomologous end-joining (NHEJ) mechanism. In this process, activation-induced cytidine deaminase (AID) is clearly required, but the precise mechanism of its action is not certain. A widely accepted model is that AID initiates CSR by deamination of cytidine residues in the Ig S regions to uracils; the resulting guanosine/uracil mismatches are recognized by uracil–DNA glycosylase and excised, ultimately leading to DNA double strand breaks (DSBs; references 1–4). An alternative model is that AID deaminates cytidines in specific mRNA molecules, and edited mRNAs encode an endonuclease that cleaves S regions, producing DSBs (5). In either model, recognition and repair of these DSBs are critical for successful completion of CSR.

The ataxia telengiectasia (AT) mutated (ATM) protein is known to play a critical role in early events of sensing and responding to DNA damage induced by insults such as ionizing radiation. The ATM protein is a member of a family of phosphatidylinositol 3-kinase–related proteins that are involved in cellular functions, including cell cycle regulation, telomere length monitoring, meiotic recombination, and DNA repair (6). In the presence of DNA damage, ATM phosphorylates a variety of protein targets, including p53 (7–9), CHK2 (10, 11), MDM2 (12, 13), BRCA1 (14, 15), and NBS1 (16–18), and activates multiple signal transduction pathways (19, 20).

The precise mechanism of ATM activation in response to DSBs is unknown but recent evidence suggests that in the absence of DNA damage, ATM is held inactive as a dimer, distributed throughout the nucleus (21). Generation of DSBs induces rapid intermolecular autophosphorylation of serine 1981 that causes dimer dissociation and allows accessibility of substrates to the ATM kinase domain (21). Lee and Paull recently reported that a complex containing Mre11, Rad50, and Nbs1 proteins stimulates the kinase activity of ATM by facilitating the stable binding of substrates (22). Visualization of ATM after DNA damage showed nuclear aggregates of ATM staining, which colocalized with foci of two proteins previously shown to localize to sites of DNA damage: NBS1 and the phosphorylated form of H2AX, known as γ-H2AX (23). Perkins et al. used chromatin immunoprecipitation to show that ATM also localizes to breaks associated with V(D)J recombination, both in the Igκ locus in a pre–B cell line, and in the TCRα locus in primary mouse thymocytes (24). These observations suggest that ATM may play a functional role in T and B cell V(D)J recombination. Consistent with this view, the absence of ATM in AT patients or in genetically engineered ATM-knockout mice results in lymphomas caused by aberrant V(D)J recombination and translocation in developing thymocytes (25–30), probably reflecting failure of normal recombination repair. The observed abnormalities in expression of switched Ig isotypes and alterations in S–S junction sequences in humans with ATM defects (31–34) suggest that ATM may also participate in Ig isotype switching. We have used a mouse model of ATM deficiency to study the role of ATM in Ig class switching, and have identified and characterized a defect in CSR that is intrinsic to B cells and suggests a role of the *Atm* gene product in DNA DSB recognition and/or repair during CSR.

Materials and Methods

Mice. $Atm^{-/-}$ mice were generated by introducing a truncation mutation into the gene at nucleotide 5790 (27). Progeny of heterozygous matings were genotyped by PCR (35). All mice used in this study were 7–12-wk-old, and $Atm^{+/+}$ littermates were used as controls. All animal experiments were approved by the National Cancer Institute Animal Care and Use Committee.

In Vivo Immunization. Mice were immunized i.p. with 100 μg TNP-KLH in Imject alum (Pierce Chemical Co.), and serum was collected on day 0 before immunization and on days 7, 14, 21, and 39 after immunization. Mice were boosted in the same manner on day 40, and serum was collected on day 8. To assay Ag-specific IgA responses, mice were immunized via intragastric instillation with 1 mg TNP-KLH and 10 μg cholera toxin (List Biological Laboratories, Inc.) in 0.2 M $NaHCO_3$. Mice were boosted in the same manner on day 22, and serum was collected on day 4 after rechallenge. Total and Ag-specific serum Ig were assayed by ELISA.

Ab Detection by ELISA. Total IgA, IgG1, IgG2a, IgG2b, IgG3, IgM, or IgE were captured with purified goat anti–mouse IgA, IgG1, IgG2a, IgG2b, IgG3, IgM, or IgE (Southern Biotechnology Associates, Inc.) and detected with horseradish peroxidase (HRP)–conjugated goat anti–mouse α, γ1, γ2a, γ2b, γ3, or μ (Southern Biotechnology Associates, Inc.) or biotinylated rat anti–mouse IgE, and HRP-conjugated streptavidin (Southern Biotechnology Associates, Inc.). To measure Ag-specific Ig, plates were coated with 2.5 μg/well TNP-OVA, and Ig was detected with HRP-conjugated anti-α, μ, γ1, γ2a, γ2b, or γ3. In all cases, wells were developed with ABTS Microwell Peroxidase Substrate System (Kirkegaard & Perry Laboratories), and OD was measured at 405 nm. Titers were determined by interpolation of the dilution of serum that gave a 50% OD of the maximum absorbance achieved.

Purification and In Vitro Activation of B Cells. Enriched populations of splenic B cells were obtained using magnetic CD19 beads according to the manufacturer's instructions (Miltenyi Biotec). 2×10^5 cells were cultured in 24-well flat-bottom plates in 1 ml of complete medium consisting of RPMI 1640 (Biowhitaker) supplemented with 10% fetal calf serum (Biofluids), 1% sodium pyruvate, 1% nonessential amino acids, 0.5% L-glutamine, 5×10^{-5} M 2-mercaptoethanol, 100 U/ml penicillin, and 100 μg/ml streptomycin and incubated at 37°C in a humidified atmosphere containing 5% CO_2. To induce specific isotype switching, B cells were stimulated with the following: for IgE, IgG1, IgG2a, and IgM, 2.15 μg/ml mouse membrane CD40 ligand (CD40L; provided by M. Kehry, Idec Pharmaceuticals, San Diego, CA; reference 36) and 1,000 U/ml recombinant mouse IL-4 (prepared from a baculovirus expression system in our laboratory); for IgG2b and IgG3, 15 μg/ml LPS (Sigma-Aldrich); and for IgA, 2.15 μg/ml CD40L, 1,000 U/ml IL-4, 150 U/ml IL-5, 10 ng/ml TGF-β (provided by A. Roberts, National Institutes of Health, Bethesda, MD), and 3 ng/ml anti-IgD dextran (a gift from C. Snapper, Uniformed Services University of the Health Sciences, Bethesda, MD). Supernatants were harvested on day 6 for quantitation of Ig by ELISA.

Surface Ig Expression. Resting splenic B cells were isolated and stimulated to induce IgG1/IgE production as described before and cells were harvested at varying time points after activation. Surface IgG1 expression was detected with biotin-conjugated goat anti–mouse IgG1 Ab and CyChrome conjugate (BD Biosciences). Surface IgE was detected with FITC-conjugated rat anti–mouse IgE mAb R1.E4 (provided by C. Snapper). This Ab recognizes an IgE epitope that is masked when IgE is bound to FcεRII; therefore, it reacts with intrinsic transmembrane IgE, but not cytophilic IgE, and can be used for quantitation of IgE-producing B cells. The specificity of anti-IgG1 and anti-IgE staining was verified by demonstrating that staining with each reagent was specifically inhibited by unlabeled Ab specific for the corresponding isotype. Samples were analyzed on a Becton Dickinson FACScan, and data were analyzed with CELLQuest software.

CFSE Staining. Cells were washed and resuspended at 10^7 cells/ml in PBS at room temperature. An equal volume of 10 μM CFSE (Molecular Probes) in PBS was added to the cell suspension, which was immediately vortexed and incubated for 8 min at room temperature. Unbound dye was quenched by the addition of an equal volume of FCS, and cells were washed three times with ice-cold complete medium. Cells were cultured under the conditions described before to induce class switching, harvested at various time points after activation, and analyzed using a Becton Dickinson FACScan.

Quantitative Real-Time RT-PCR. RNA was extracted from cultured cells with TRIzol, as described by the supplier (Invitrogen). Approximately 1 μg RNA was used to generate cDNA using SuperScript II reverse transcriptase and random hexamers (Invitrogen). The resulting cDNA was used in quantitative real-time PCR reactions using an ABI 7900HT machine and ABI 2X SYBR green Master Mix. Amplification of GAPDH was used for sample normalization, and quantification of gene expression relative to GAPDH was performed using the ΔΔCT methods as described by the manufacturer (Sequence Detector User Bulletin 2; Applied Biosystems). PCR primers used for these analyses are as follows: germline IgG1, Gγ1, 5′-TCGAGAAGCCTGAGGAATGT-3′ and 5′-ATAGACAGATGGGGGTGTCG-3′; germline IgE, Gε, 5′-CTGGCCAGCCACTCACTTAT-3′ and 5′-CAGTGCCTTTACAGGGCTTC-3′; productive IgG1, Pγ1, 5′-TCGAGAAGCCTGAGGAATGT-3′ and 5′-ATAGACAGATGGGGGTGTCG-3′; productive IgE, Pε, 5′-TTGGACTACTGGGGTCAAGG-3′ and 5′-CAGTGCCTTTACAGGGCTTC-3′; GAPDH, 5′-TGCACCACCAACTGCTTAG-3′ and 5-CGCCGCTAGAGGTGAAATTCT-3′. All quantitative real-time PCR reactions were performed two times in triplicate.

Digestion–Circularization-PCR (DC-PCR). Genomic DNA was isolated from cultured B cells using a DNA isolation kit (QIAGEN) according to the manufacturer's instructions. 1 μg DNA was digested with EcoRI (New England Biolabs, Inc.) overnight and 100 ng was ligated overnight with T4 DNA ligase in a volume of 50 μl (New England Biolabs, Inc.). Ligated DNA was subjected to two rounds of PCR using nested primer pairs for Sμ–Sγ1, Sμ–Sε, and nicotinic acetylcholine receptor (nAChR) DC-PCR. Primers for the first round of PCR were as follows: Sμ–Sγ1, 5′-GAGCAGCTACCAAGGATCAGGGA-3′ and 5′-CTTCACGCCACTGACTGACTGAG-3′; Sμ–Sε, 5′-CGGGTATTGGAAAATAATTGAATG-3′ and 5′-GCAGAGCATCCTCACATACA-3′; and nAChR, 5′-GCAAACAGGGCTGGATGAGGCTG-3′ and 5′-GTCCCATACTTAGAACCCCAGCG-3′. For Sμ–Sγ1 and nAChR amplification, conditions were 5 cycles at 94°C for 1 min, 65°C for 1 min, and 72°C for 2 min; and 30 cycles at 94°C for 1 min, 68°C for 1 min, and 72°C for 2 min. Amplification conditions for Sμ–Sε were 35 cycles at 94°C for 1 min, 55°C for 1.5 min, and 72°C for 2 min. Primers for the second round of PCR were as follows: Sμ–Sγ1, 5′-GGAGACCAATAATCAGAGGGAAG-3′ and 5′-GAGAGCAGGGTCTCCTGGGTAGG-3′; Sμ–Sε, 5′-GTCCTTCAATTTCTTACATAACC-3′ and 5′-ATGCAGGATAGACCCCAGAC-3′; and nAChR, 5′-GGACTGCTGTGGGTTTCACCCAG-3′ and 5′-GCCTTGCTTGCTTAAGACCCTGG-3′. PCR conditions for Sμ–Sγ1 and nAChR were the same as for the first round, and conditions for Sμ–Sε were 30 cycles at 94°C for 1 min, 57°C for 1.5 min, and 72°C for 2 min.

Switch Junction Analysis. Sμ–Sγ1 junctions were amplified from genomic DNA from CD40L–IL-4–stimulated B cells using Expand long template PCR system (Roche) and primers 5μ3, 5′-AATGGATACCTCAGTGGTTTTTAATGGTGGGTTTA-3′ and γ1-R, 5′-CAATTAGCTCCTGCTCTTCTGTGG-3′. Amplification conditions were 35 cycles at 95°C for 30 s, 58°C for 45 s, and 72°C for 2 min and 30 s. PCR products (500–1,000 bp) were gel extracted, cloned using TA cloning kit (Invitrogen), and sequenced using 5μ3 and γ1-R primers. Sequence analysis was performed using DNASTAR software.

Hypermutation Analysis. For V_κOx1 genes, three *Atm*-deficient mice were immunized i.p. with phenyloxazolone coupled to chicken serum albumin in adjuvant. Mice were killed 4 d after the secondary injection, and spleens were removed. B cells that bound phycoerythrin-labeled antibody to B220 (BD Biosciences) and fluorescein-labeled peanut agglutinin (PNA; E-Y laboratories) were isolated by flow cytometry. DNA from $B220^+PNA^+$ cells was amplified using primers that included 190 bases of 5′ intron sequence, the V_κOx1 coding sequence, and the J_κ5 gene segment (37). Amplified products were cloned into pBluescript and sequenced. For S_μ regions, one $Atm^{-/-}$ mouse and littermate control were immunized with TNP-KLH and killed after the second injection. DNA from $B220^+PNA^+$ spleen cells was amplified using primers for a 561-bp region located upstream of the S_μ core region (38) and sequenced. PCR error was determined by sequencing similar regions from nonactivated B cells (0.4×10^{-4} mutations/bp; 1 mutation per 24,963 nucleotides). Two-sided p-values were determined to compare frequencies.

Results

Ig Production Is Impaired in Atm-deficient Mice. It has been reported that AT patients have deficiencies in serum IgA, IgE, IgG2, and IgG4 levels (31, 32, 39–42). To assess the role of ATM in Ig class switching, basal serum Ig levels of different isotypes were therefore assessed in unimmunized $Atm^{-/-}$ mice. Levels of IgA, IgG2b, and IgM were not significantly different in $Atm^{-/-}$ and $Atm^{+/+}$ (Fig. 1 A). However, $Atm^{-/-}$ mice had significantly lower levels of IgG1, IgG2a, and IgG3 than wild-type mice (Fig. 1 A). IgE was undetectable in both normal and mutant mice (unpublished data). The immune competence of $Atm^{-/-}$ mice for T cell–dependent (TD) antibody responses was assessed by measuring the in vivo response to challenge with TNP-KLH in alum. There was no difference in Ag-specific IgM responses of $Atm^{-/-}$ and $Atm^{+/+}$ mice (Fig. 1 B). In contrast, the Ag-specific IgG1 response in $Atm^{-/-}$ mice was 16–38-fold lower than the WT controls at all the time points tested (Fig. 1 C). To detect production of other iso-

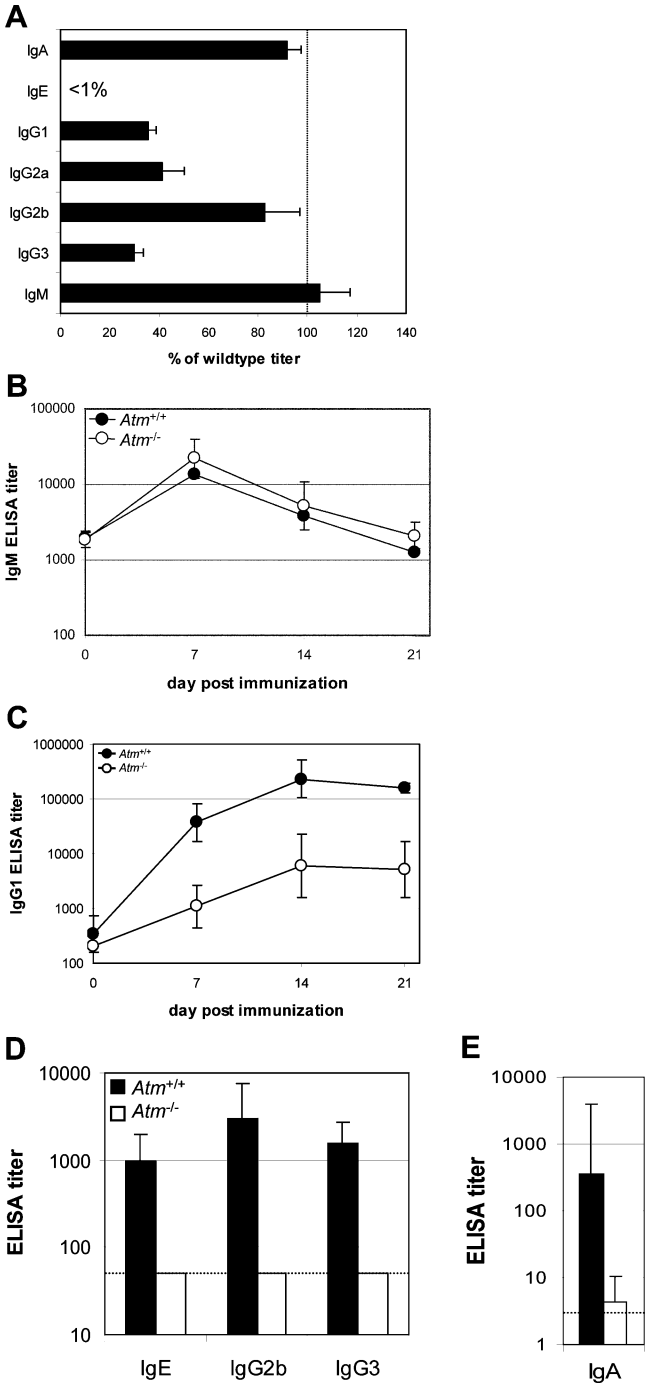

Figure 1. Impaired Ig production in $Atm^{-/-}$ mice. (A) Sera from eight *Atm*-deficient mice and littermate controls were assayed for total Ig levels by ELISA. IgE was undetectable by ELISA in sera from unimmunized mice. Results are displayed as the mean ± SEM $Atm^{-/-}$ titer as a percentage of the $Atm^{+/+}$ controls. (B–D) Three $Atm^{-/-}$ mice and their WT littermates were immunized with TNP-KLH/Alum i.p., and serum was collected at the indicated time points. Serum levels of Ag-specific IgM (B) and IgG1 (C) were assayed by ELISA; data points represent the geometric mean ± geometric SEM of the ELISA titers. (D) Mice received a second immunization of TNP-KLH/Alum 40 d after the first immunization, and serum was collected after 8 d. Serum levels of total IgE and Ag-specific IgG2b and IgG3 were assayed by ELISA, and data points are displayed as the mean ± SD $Atm^{-/-}$ titer as a percentage of the $Atm^{+/+}$ controls. The dotted line indicates the limit of detection. IgE, IgG2b, and IgG3 were undetectable in $Atm^{-/-}$ mice. Results are representative of two independent experiments. (E) Serum levels of Ag-specific IgA were measured in mice (five per group) immunized with TNP-KLH p.o., and serum was collected 4 d after the second immunization.

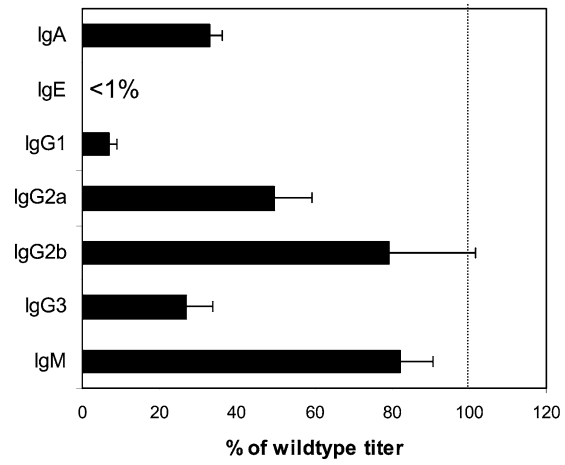

Figure 2. Defective Ig production in $Atm^{-/-}$ B cells activated in vitro. $CD19^+$ B cells were isolated from the spleens of $Atm^{-/-}$ and WT mice and cultured with CD40L and IL-4 (IgG1, IgG2a, and IgM), CD40L, IL-4, IL-5, TGF-β, and anti-IgD dextran (IgA) or LPS (IgG2b, IgG3). Results are displayed as the mean of three to four experiments ± SEM $Atm^{-/-}$ titer as a percentage of the $Atm^{+/+}$ controls.

types, the mice received a second immunization of Ag, and serum was collected at day 8 after rechallenge. Significant Ag-specific IgG2b and IgG3 responses were detected in WT mice, but not in *Atm*-deficient mice (Fig. 1 D). Levels of Ag-specific IgA, IgE, and IgG2a were low or undetectable in all mice tested in response to this immunization (unpublished data). Because we could not detect Ag-specific IgE in response to immunization (unpublished data), we measured total IgE serum levels at day 8 after a secondary immunization. Levels of IgE were low or undetectable in unimmunized mice (not depicted), but increased significantly after immunization of WT mice (Fig. 1 D). In contrast, an IgE response was not detected in $Atm^{-/-}$ mice. To detect Ag-specific IgA, mice were immunized via gastric feeding to stimulate a mucosal response. Ag-specific IgA was found in WT mice at day 4 after a secondary immunization, whereas it was low or undetectable in KO mice (Fig. 1 E). These results suggest that $Atm^{-/-}$ mice have a defect in CSR after immunization with a TD Ag.

In Vitro Secretion of Class-switched Isotypes Is Defective in Atm-deficient B Cells. To examine the intrinsic ability of $Atm^{-/-}$ B cells to undergo CSR in vitro, splenic B cells were cultured with various polyclonal B cell activators (43) and levels of IgA, IgG1, IgG2b, IgG3, IgE, and IgM were measured in day 6 supernatants. The unswitched IgM response of $Atm^{-/-}$ B cells was minimally reduced relative to WT controls (82% of control titers), whereas switched isotypes were affected to different degrees (Fig. 2). Most affected was the IgE response, which was undetectable in $Atm^{-/-}$ B cell

cultures (<1% of WT responses), and IgG1, for which *Atm*$^{-/-}$ B cells produced 7% of the levels in WT B cell cultures. IgA, IgG2a, and IgG3 were all significantly lower in *Atm*$^{-/-}$ cultures. IgG2b responses were not significantly reduced, in contrast with the reduction in Ag-specific IgG2b production observed in vivo (Fig. 1 D). To determine whether the decrease in IgG1 and IgE secretion by in vitro–stimulated *Atm*-deficient B cells resulted from an altered frequency of cells undergoing CSR or reflected only decreased production of Ig per isotype-switched cell, we examined surface Ig by flow cytometry. After 4 d of in vitro activation, surface IgG1 was expressed by 38% of *Atm*$^{+/+}$ B cells, and surface IgE was expressed by 5.3% of *Atm*$^{+/+}$ B cells (Fig. 3). In contrast, IgG1 was expressed by only 9% of *Atm*$^{-/-}$ B cells and there was little or no detectable expression of IgE by *Atm*$^{-/-}$ B cells. Thus, the observed in vivo and in vitro deficiencies in Ig secretion in *Atm*$^{-/-}$ mice and cells appear to be due to an intrinsic B cell defect in CSR.

The Ig CSR Deficiency in Atm$^{-/-}$ *B Cells Is Not Due to Altered Clonal Expansion.* The generation of class-switched B cells is dependent on cellular proliferation through at least two effects. First, it has been reported that the CSR process itself requires cellular proliferation (44). In addition, B cells undergo clonal expansion after CSR, and the number of class-switched cells detected after a B cell response will be determined by the degree of this clonal expansion. To determine whether the reduced switching observed in *Atm*$^{-/-}$ B cells could be explained by a defect in cell proliferation, we combined cytoplasmic dye dilution with flow cytometric staining of surface Ig isotypes to measure clonal expansion of switched and nonswitched cells. In the absence of surface IgE expression by *Atm*$^{-/-}$ B cells (Fig. 3), it was not possible to assess the effect of *Atm* deletion on

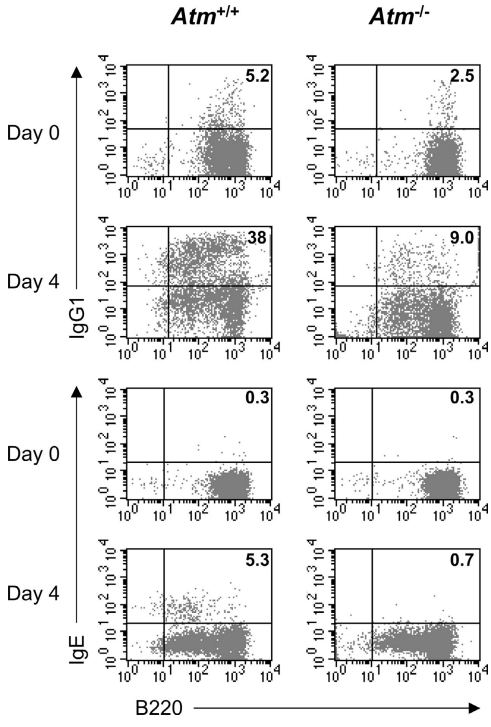

Figure 3. Surface Ig expression of IgG1 and IgE isotypes on in vitro–stimulated wild type and *Atm*$^{-/-}$ B cells. Cells were harvested after 4 d of in vitro stimulation with CD40L and IL-4, and flow cytometric analysis was used to determine surface IgG1 and IgE expression. Numbers on the dot plots show the percentage of switched cells as a proportion of B220^{+} B cells. Results are representative of four independent experiments.

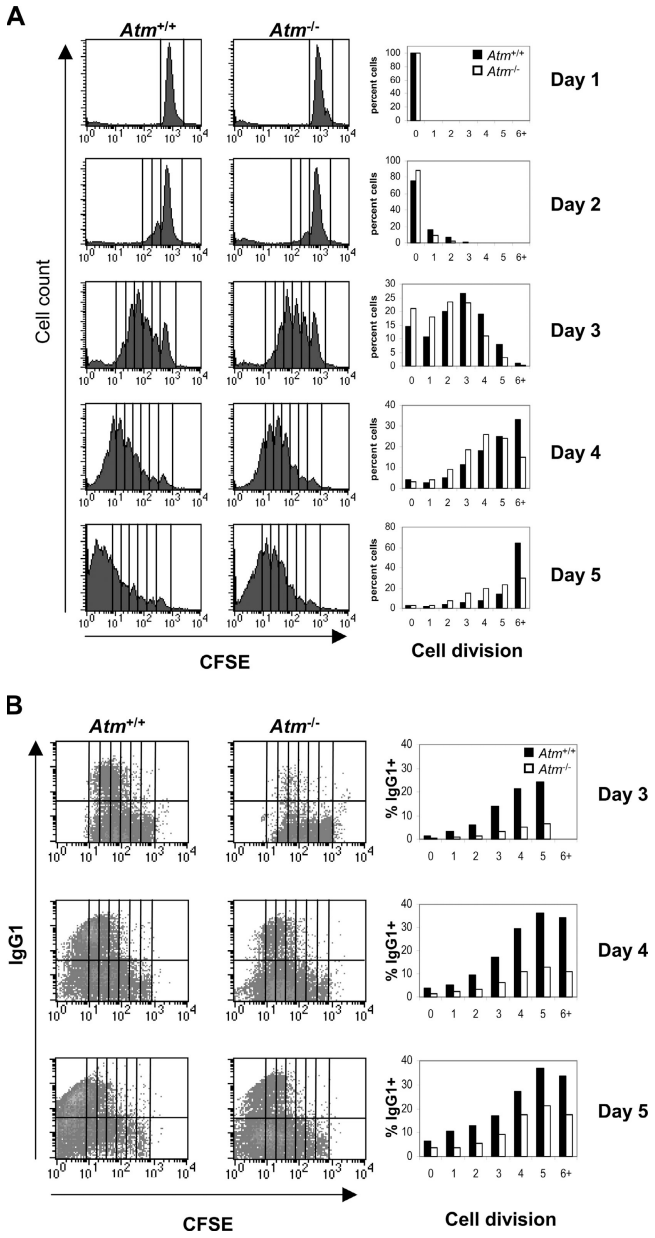

Figure 4. Clonal expansion of IgG1-switched B cells. CFSE-stained resting B cells were stimulated in vitro with CD40L and IL-4 for 3–6 d and counterstained with goat anti–mouse IgG1 as described in Materials and Methods. (A) CFSE staining profiles of *Atm*$^{+/+}$ and *Atm*$^{-/-}$ B cells are presented in the first two columns. The third column shows the percentage of recovered *Atm*$^{-/-}$ and *Atm*$^{+/+}$ cells that have undergone the indicated number of cell divisions. (B) Two-color flow cytometric profiles indicate IgG1 expression on CFSE stained cells. The percentage of B cells expressing IgG1 is indicated for *Atm*$^{+/+}$ B cells and *Atm*$^{-/-}$ B cells that have undergone the indicated numbers of cell divisions. Results are representative of three independent experiments.

clonal expansion of IgE-switched cells. However, it was possible to carry out a comparison of IgG1 switching and clonal expansion in $Atm^{+/+}$ and $Atm^{-/-}$ B cells. Resting splenic B cells from $Atm^{-/-}$ and control mice were labeled with CFSE and activated in vitro with CD40L and IL-4. At multiple time points after stimulation, cells were harvested and counterstained for surface IgG1 expression. Dilution of intracellular CFSE staining allowed quantitative assessment of cell division, whereas surface Ig staining allowed identification of IgG1-switched B cells. A modest decrease in cell division was observed in the response of $Atm^{-/-}$ B cells to CD40L and cytokines, as reflected by a higher proportion of $Atm^{-/-}$ cells that had undergone fewer cell divisions as compared with $Atm^{+/+}$ cells (Fig. 4 A). In both $Atm^{+/+}$ and $Atm^{-/-}$ B cells, surface expression of IgG1 increased with increasing number of cell divisions (Fig. 4 B). Moreover, the percentage of IgG1 positive B cells was two- to threefold greater in the population of $Atm^{+/+}$ B cells that had undergone three to six divisions than for the population of $Atm^{-/-}$ B cells that had undergone an identical number of divisions. These results indicate that a class switch defect, independent of differences in clonal expansion, is the predominant determinant of decreased IgG1-switched cells seen in $Atm^{-/-}$ mice.

Germline Transcripts Are Normal, but Productive Transcripts Are Impaired in Atm-deficient B Cells. To assess the molecular mechanisms involved in the defective CSR to IgG1 and IgE observed in $Atm^{-/-}$ B cells, we examined the expression of germline (Gγ1, Gε) and productive (Pγ1 and Pε) transcripts by real-time RT-PCR. Resting B cells from $Atm^{-/-}$ and control spleens were activated in vitro with CD40L and IL-4, and total RNA was isolated from cells harvested at days 3 and 6. Both Gγ1 and Gε transcripts peaked on day 3 for stimulated B cells from WT cells, whereas Pγ1 and Pε transcripts peaked at day 6 (Fig. 5 and not depicted). Similar amounts of Gγ1 and Gε transcripts were induced in $Atm^{-/-}$ B cells and controls (Fig. 5) indicating that $Atm^{-/-}$ B cells were competent to respond to signals delivered by CD40L and cytokines. In contrast, the expression of Pγ1 and Pε transcripts in $Atm^{-/-}$ B cells was markedly reduced, with amplified Pγ1 transcripts being 14-fold lower and Pε transcripts 60-fold lower than normal controls. These data suggest that ATM has a role downstream of germline transcription.

Atm-deficiency Reduces Class Switching at the Level of DNA Recombination. To determine directly whether the decrease in isotype switching occurs at the level of DNA recombination, we used a quantitative DC-PCR assay (45) to measure actual switch recombination. In B cells that have undergone CSR, 5′ Sμ sequences are contiguous with 3′ Sγ1 or Sε on the recombined IgH allele. After EcoRI digestion of genomic DNA, Sμ and Sγ1 or Sμ and Sε sequences therefore reside on the same DNA fragment if switching to that isotype has occurred. To detect these fragments, EcoRI-digested genomic DNA was ligated under conditions that promote circularization, and the region spanning the ligated EcoRI junctions was amplified by a PCR strategy that produces PCR products of uniform size, independent of where recombination took place within the S region (45). Primers specific for a control EcoRI fragment that does not undergo rearrangement (nAChR) were

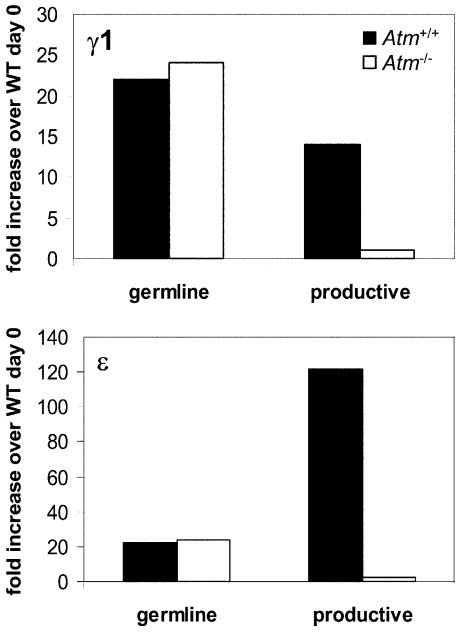

Figure 5. Real-time RT-PCR analysis of germline and productive IgG1 and IgE transcripts in $Atm^{-/-}$ B cells activated in vitro. Total RNA was isolated from B cells activated in vitro, and quantitative real-time RT-PCR was performed as described in Materials and Methods. Germline transcripts were measured at day 3 of culture and productive transcripts were measured at day 6 of culture. The data were normalized to GAPDH and presented as the increase in transcript level over unstimulated wild-type B cells. The data shown are representative of two independent experiments.

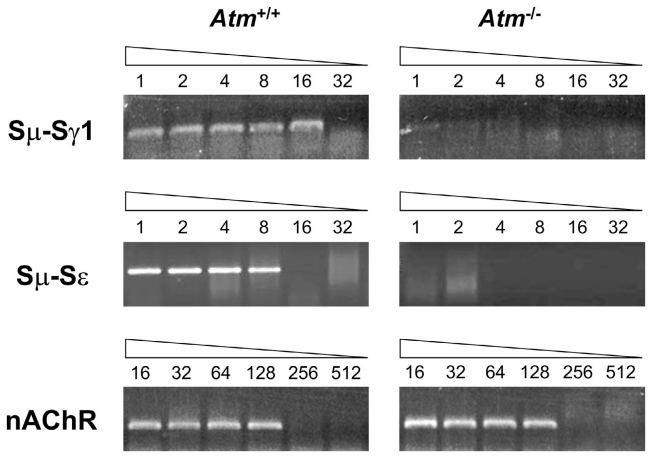

Figure 6. DC-PCR analysis of genomic switch recombination in wild type and $Atm^{-/-}$ B cells. Genomic DNA was isolated from B cells activated in vitro for 6 d, digested with EcoRI, and ligated with T4 DNA ligase. Twofold serial dilutions were used as a template for DC-PCR using primers specific for the recombined S regions. nAChR levels were also determined by DC-PCR to control for equal template loading. The results shown are representative of two independent experiments.

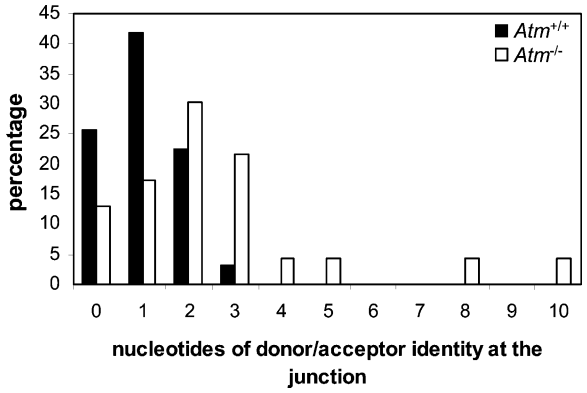

Figure 7. Sμ–Sγ1 switch recombination junctions from $Atm^{-/-}$ B cells. Histogram depicting the percentage of sequences with the indicated length of microhomology at Sμ–Sγ1 junctions. Overlap was determined by identifying the longest region at the switch junction of perfect uninterrupted donor/acceptor identity.

used to control for DNA input and efficiency of digestion and circularization. DC-PCR analysis indicated that the frequency of Sμ–Sγ1 switch recombination in $Atm^{-/-}$ B cells was at least 16-fold lower than in WT B cells (Fig. 6). Sμ–Sε recombination in $Atm^{-/-}$ B cells was at least eightfold lower than in WT B cells. Thus, the reduction in isotype switching observed in *Atm*-deficient B cells reflects a defect at the level of DNA recombination.

Analysis of CSR Junctions from Atm-deficient B Cells. Although the efficiency of CSR is decreased in the absence of ATM, some cells do succeed in producing IgG1 in response to CD40L and IL-4. To determine whether these CSR junctions were altered in the absence of ATM, we compared IgG1 CSR junctions from $Atm^{-/-}$ ($n = 23$ junctions) and WT ($n = 31$ junctions) B cells (Fig. 7). We found a significant increase in the amount of donor–acceptor (Sμ–Sγ1) homology at the switch junctions from $Atm^{-/-}$ B cells; the average length of overlap was 2.6 ± 0.5 bp in the $Atm^{-/-}$ and 1.2 ± 0.2 bp in control B cells ($P = 0.01$, Student's *t* test). Thus, ATM function may affect the preference for sequence homology, as well as overall efficiency of CSR.

Analysis of Hypermutation in V_κ and S Regions from Atm-deficient B Cells. To determine the effect of ATM deficiency on another AID-dependent B cell–specific process, we analyzed somatic hypermutation in V_κOx1 genes and switch regions. For selected V_κOx1 genes from

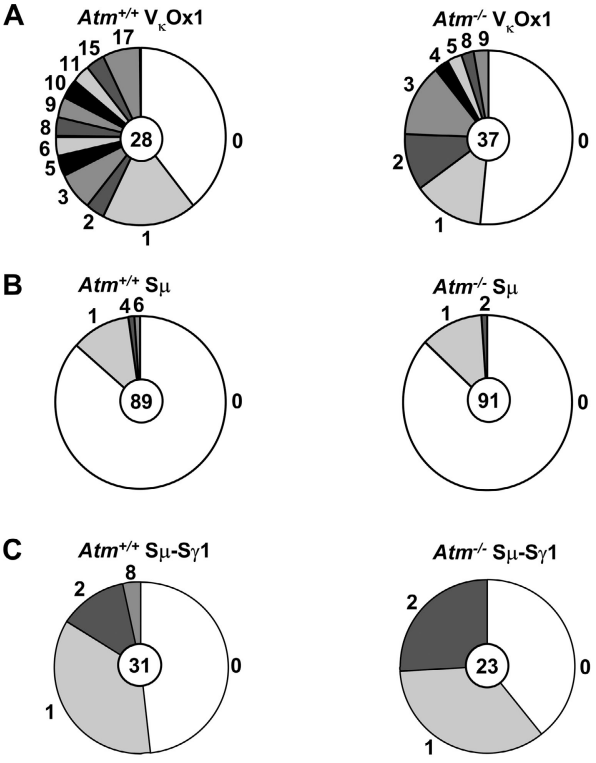

D

	$Atm^{+/+}$	$Atm^{-/-}$	P-value
V_κOx1	85 X 10^{-4} mut/bp (111/13,048)	31 X 10^{-4} mut/bp (54/17,242)	$<10^{-3}$
	49% G:C	55% G:C	0.77
Sμ	4 X 10^{-4} mut/bp (20/49,929)	2.5 X 10^{-4} mut/bp (13/51,051)*	0.23
	60% G:C	40% G:C	0.74
Sμ-Sγ1	87 X 10^{-4} mut/bp (27/3,100)	87 X 10^{-4} mut/bp (20/2,300)	1
	47% G:C	70% G:C	0.75

Figure 8. Hypermutation analyses in V_κ and S regions from *Atm*-deficient mice. (A) Mutation in rearranged V_κOx1 genes. The total number of clones analyzed is shown in the center of each circle. The pie segments represent the proportion of clones that contained the specified number of mutations indicated. (B) Mutation in upstream S_μ regions. (C) Mutations near the Sμ–Sγ1 junctions (±50 bp). (D) Frequencies of mutation. The number of mutations and bases sequenced are shown in parentheses. Percent of mutations at G and C bases was calculated after correction for base composition. p-values compare the data for $Atm^{+/+}$ to $Atm^{-/-}$ clones. *, frequency of $Atm^{-/-}$ S_μ clones is significantly higher than PCR error ($P = 0.045$).

PNA^+B220^+ spleen cells from immunized mice (Fig. 8 A), the frequency of mutation per basepair was lower in $Atm^{-/-}$ clones (31×10^{-4}) compared with $Atm^{+/+}$ clones (85×10^{-4}; $P < 10^{-3}$, Fisher's exact test). However, the spectra of base changes in $Atm^{-/-}$ clones (53 mutations; 55% at G:C pairs) was similar to that from $Atm^{+/+}$ clones (111 mutations; 49% at G:C pairs; $P = 0.77$; Fig. 8 D). For unselected S regions, the frequency of mutation per basepair was not significantly different between the two groups of clones in either upstream Sμ regions from PNA^+B220^+ spleen cells ($Atm^{+/+}$, 4×10^{-4}; $Atm^{-/-}$, 2.5×10^{-4}; $P = 0.22$; Fig. 8 B) or within 50 nucleotides from the Sμ–Sγ1 junctions from CD40L–IL-4–stimulated spleen cells ($Atm^{+/+}$, 87×10^{-4}; $Atm^{-/-}$, 87×10^{-4}; Fig. 8 C). There was also no significant difference in the frequency of substitutions at G:C vs. A:T base pairs between the two groups of clones (Fig. 8 D).

Discussion

ATM plays a critical role in pathways for repair of DNA DSBs induced by insults such as gamma irradiation (46). Studies have also indicated that Ig class switching involves induction of DNA breaks and their resolution by NHEJ. Thus, animals or cells that lack protein components of the NHEJ pathway, such as Ku80, Ku70, or DNA-PKcs, have major defects in class switching (47–49). To assess the role that ATM may play in sensing and responding to DNA DSBs generated during Ig heavy chain CSR, we examined the in vivo and in vitro antibody responses of *Atm*-deficient mice. *Atm*-deficient mice have reduced basal serum levels of several IgG isotypes and generate markedly reduced titers of Ag-specific IgG1 and total IgE, as well as significant decreases in Ag-specific IgA, IgG2b, and IgG3 compared with WT controls after immunization with TD Ag. These findings are parallel to the defect in class switching that is observed in AT, where it is associated with a susceptibility to recurrent infections (31, 32, 39–42).

Antibody responses to TD Ags require both intact B cell function and T cell help. Although there is evidence for T cell defects in AT patients (50, 51), our preliminary experiments failed to identify a defect in T helper function in $Atm^{-/-}$ mice as reflected by normal polarized maturation to Th1 or Th2 cells producing IFN-γ or IL-4, respectively (unpublished data). Therefore, further studies focused on an analysis of intrinsic B cell function in *Atm*-deficient mice. In vitro activation of resting B cells with CD40L, LPS, or anti-IgD in combination with appropriate cytokines revealed a decrease in production of multiple class-switched Ig isotypes by $Atm^{-/-}$ as compared with WT B cells. Flow cytometric analysis of the cultured cells demonstrated that there were fewer cells undergoing CSR in the absence of ATM. Thus, when surrogate Th signals were provided in vitro, $Atm^{-/-}$ B cells were markedly deficient in switching to IgG1 and IgE, and significantly reduced in switching to IgA, IgG2a, and IgG3 as well. These findings suggested that the observed defects in Ig class switching are intrinsic to $Atm^{-/-}$ B cells. Defects in polyclonal activation of B cells from AT patients have also been shown to be B cell intrinsic (52).

The production and secretion of Ig isotypes other than IgM are accomplished by a deletional recombination event that brings a downstream C_H gene into proximity with V(D)J elements. All intervening DNA, consisting of the C_H genes located between the V(D)J locus and the targeted C_H gene, is looped out and deleted. This switch recombination is preceded by the production of a sterile germline transcript from the C_H gene that is to be recombined. Germline transcription appears to be essential for CSR. The germline transcript may provide the DNA recombinatorial machinery with access to the chromosomal region containing the C_H gene to be expressed (53, 54) or the transcript itself may participate in CSR by binding to the template strand of the switch region, promoting a structure that is accessible to the recombination machinery (4, 55). We evaluated the role of clonal expansion of switched and nonswitched B cells by flow cytometry and assayed Gγ1, Gε, Pγ1, and Pε mRNA by real-time RT-PCR. Normal levels of Gγ1 and Gε transcription were detected in $Atm^{-/-}$ mice, indicating that $Atm^{-/-}$ B cells are capable of being activated by CD40L and IL-4 and that the CSR defect does not result from impaired germline transcription. However, a substantial reduction was observed in Pγ1 and Pε expression, suggesting that $Atm^{-/-}$ mice are defective in μ–γ and μ–ε switch recombination and/or in the transcription of successfully recombined IgH genes. Analysis of genomic DNA by DC-PCR demonstrated a defect at the level of DNA recombination. When clonal expansion was measured by dye dilution in IgG1 class switched and unswitched B cells, it was found that a class switch defect, independent of clonal expansion, is the predominant cause of the observed deficiency in switched $Atm^{-/-}$ B cells. These findings suggest a functional role of the *Atm* gene product in switch recombination.

Several studies have suggested that ATM may be involved in DNA damage repair, cell cycle regulation, and meiotic recombination, all of which have in common the response to DNA DSBs. The *Atm* gene product shows sequence similarity to the PI 3-kinase, and the catalytic subunit of DNA-dependent protein kinase (DNA-PKcs). The DNA–PK complex is thought to be activated by DNA DSBs, resulting in binding of the Ku70–Ku80 heterodimer followed by recruitment of DNA-PKcs to the complex. Although $Atm^{-/-}$ mice resemble mice deficient in components of the Ku–DNA–PK complex in being radiosensitive and immunodeficient, the phenotypes are different in important respects. In the immune system, the Ku–DNA–PK complex is required for both V(D)J rearrangement and Ig CSR, and mice deficient in any of these components have been reported to have defects in lymphocyte development. In contrast, $Atm^{-/-}$ mice are competent for V(D)J rearrangement as reflected in the development of mature T and B cell receptor repertoires. However, it is of interest that many thymic lymphomas as well as nontransformed T cells in these mice harbor abnormal translocations of the T cell receptor α/δ locus (30), suggesting that there may in fact

be abnormalities in T cell receptor rearrangement in the absence of the *Atm* product. Although ATM appears to be required for optimal CSR to multiple isotypes, including a marked influence on IgG1 responses, DNA-PKcs–deficient B cells have been reported to be competent for class switching to IgG1, but not other isotypes (56). Collectively, these findings suggest that ATM and DNA–PK mediate distinct but related functions in the molecular mechanisms that underlie DNA DSB repair, V(D)J recombination, and Ig CSR. The DNA damage–response factors 53bp1 and γ-H2AX are also required for CSR but are dispensable for V(D)J recombination (57–59). The defect in CSR that is seen in B cells from 53bp1- or γ-H2AX–deficient mice is strikingly similar to that observed in *Atm*-deficient B cells in that there is no defect in C_H germline transcription but impaired CSR. The relationship between 53bp1 and ATM may be complex (60). It has been reported that phosphorylation of 53bp1 in response to DNA damage is partially, but incompletely, dependent on expression of *Atm*, suggesting that 53bp1 can be phosphorylated by ATM or other kinases, such as ATR (61, 62).

The specific role of ATM proteins in events such as Ig CSR may be related to their general function in recognition and response to DNA DSB. It has been reported that Ig class switching occurs in cells undergoing proliferation and that inhibition of DNA synthesis prevents switch recombination (63–65). Thus, it is important that any DNA breaks be resolved to be compatible with DNA synthesis and mitosis. *Atm*-deficient mice may have an abnormal DNA damage surveillance program that results in failure to repair cells with DSBs induced during the course of immune gene rearrangements, through an inability to induce cell cycle arrest until the completion of rearrangement repair. Elucidation of the components involved in this recognition should enhance our understanding of the mechanism of isotype switching.

Sequence analyses of CSR events in *Atm*-deficient B cells provided additional information regarding the function of ATM in these processes. The finding that sequence homology at Sμ–Sγ1 junctions is greater in *Atm*-deficient mouse B cells than in WT controls is consistent with a recent finding in B cells from AT patients (33), although the effect that we have observed in mice appears to be less marked than that in patients. This finding suggests that ATM may either affect the site of initial DNA breaks in switch regions or, perhaps more likely, may affect the efficiency of break repair and splicing in the process of CSR. Thus, the presence of ATM may increase overall efficiency of repair, rendering it less dependent on a facilitating role of switch region homology.

The observed decrease in CSR in *Atm*-deficient B cells could be due to reduced activity of AID, the enzyme producing strand breaks and hypermutation. Therefore, we examined switch region sequences from PNA^+ B cells and from in vitro–switched B cells and found no significant difference in the frequency of mutation between *Atm*-deficient and proficient clones. This supports a role for ATM in CSR after AID-induced lesions are introduced. There was a small but significant, approximately twofold, decrease in the frequency of somatic hypermutation in V_κOx1 genes in immunized *Atm*-deficient mice, although the types of substitutions were similar to those from WT mice. Thus, the ATM protein may not directly participate in the hypermutation pathway, but may have an indirect role in influencing the frequency of mutation. In *Atm*-deficient patients, a lower frequency of mutation in switch regions, but not in V_H genes, was observed in peripheral blood lymphocytes (34), and the basis for this difference from findings in mice is not apparent.

We thank A. Nussenzweig, K. Hathcock, and M. Vacchio for valuable comments and critical reading of this paper; J. Chiang and B. Reina-San-Martin for help with sequencing; D. Winter and D. Fu for assistance in the hypermutation analysis; G. Sanchez-Howard and the staff at Bioqual, Inc. for excellent animal care and husbandry; and S. Sharrow, L. Granger, and T. Adams for advice with flow cytometry.

The authors have no conflicting financial interests.

Submitted: 1 June 2004
Accepted: 30 September 2004

References

1. Petersen-Mahrt, S.K., R.S. Harris, and M.S. Neuberger. 2002. AID mutates *E. coli* suggesting a DNA deamination mechanism for antibody diversification. *Nature*. 418:99–103.
2. Revy, P., T. Muto, Y. Levy, F. Geissmann, A. Plebani, O. Sanal, N. Catalan, M. Forveille, R. Dufourcq-Labelouse, A. Gennery, et al. 2000. Activation-induced cytidine deaminase (AID) deficiency causes the autosomal recessive form of the Hyper-IgM syndrome (HIGM2). *Cell*. 102:565–575.
3. Muramatsu, M., K. Kinoshita, S. Fagarasan, S. Yamada, Y. Shinkai, and T. Honjo. 2000. Class switch recombination and hypermutation require activation-induced cytidine deaminase (AID), a potential RNA editing enzyme. *Cell*. 102: 553–563.
4. Nambu, Y., M. Sugai, H. Gonda, C.G. Lee, T. Katakai, Y. Agata, Y. Yokota, and A. Shimizu. 2003. Transcription-coupled events associating with immunoglobulin switch region chromatin. *Science*. 302:2137–2140.
5. Begum, N.A., K. Kinoshita, N. Kakazu, M. Muramatsu, H. Nagaoka, R. Shinkura, D. Biniszkiewicz, L.A. Boyer, R. Jaenisch, and T. Honjo. 2004. Uracil DNA glycosylase activity is dispensable for immunoglobulin class switch. *Science*. 305:1160–1163.
6. Zakian, V.A. 1995. ATM-related genes: what do they tell us about functions of the human gene? *Cell*. 82:685–687.
7. Banin, S., L. Moyal, S. Shieh, Y. Taya, C.W. Anderson, L. Chessa, N.I. Smorodinsky, C. Prives, Y. Reiss, Y. Shiloh, and Y. Ziv. 1998. Enhanced phosphorylation of p53 by ATM in response to DNA damage. *Science*. 281:1674–1677.
8. Canman, C.E., D.S. Lim, K.A. Cimprich, Y. Taya, K. Tamai, K. Sakaguchi, E. Appella, M.B. Kastan, and J.D. Siliciano. 1998. Activation of the ATM kinase by ionizing radiation and phosphorylation of p53. *Science*. 281:1677–1679.
9. Khanna, K.K., K.E. Keating, S. Kozlov, S. Scott, M. Gatei, K. Hobson, Y. Taya, B. Gabrielli, D. Chan, S.P. Lees-Miller, and M.F. Lavin. 1998. ATM associates with and phosphorylates p53: mapping the region of interaction. *Nat. Genet*. 20:

398–400.
10. McGowan, C.H. 2002. Checking in on Cds1 (Chk2): a checkpoint kinase and tumor suppressor. *Bioessays.* 24:502–511.
11. Bartek, J., J. Falck, and J. Lukas. 2001. CHK2 kinase–a busy messenger. *Nat. Rev. Mol. Cell Biol.* 2:877–886.
12. Khosravi, R., R. Maya, T. Gottlieb, M. Oren, Y. Shiloh, and D. Shkedy. 1999. Rapid ATM-dependent phosphorylation of MDM2 precedes p53 accumulation in response to DNA damage. *Proc. Natl. Acad. Sci. USA.* 96:14973–14977.
13. Maya, R., M. Balass, S.T. Kim, D. Shkedy, J.F. Leal, O. Shifman, M. Moas, T. Buschmann, Z. Ronai, Y. Shiloh, et al. 2001. ATM-dependent phosphorylation of Mdm2 on serine 395: role in p53 activation by DNA damage. *Genes Dev.* 15:1067–1077.
14. Cortez, D., Y. Wang, J. Qin, and S.J. Elledge. 1999. Requirement of ATM-dependent phosphorylation of brca1 in the DNA damage response to double-strand breaks. *Science.* 286:1162–1166.
15. Gatei, M., B.B. Zhou, K. Hobson, S. Scott, D. Young, and K.K. Khanna. 2001. Ataxia telangiectasia mutated (ATM) kinase and ATM and Rad3 related kinase mediate phosphorylation of Brca1 at distinct and overlapping sites. In vivo assessment using phospho-specific antibodies. *J. Biol. Chem.* 276:17276–17280.
16. Lim, D.S., S.T. Kim, B. Xu, R.S. Maser, J. Lin, J.H. Petrini, and M.B. Kastan. 2000. ATM phosphorylates p95/nbs1 in an S-phase checkpoint pathway. *Nature.* 404:613–617.
17. Gatei, M., D. Young, K.M. Cerosaletti, A. Desai-Mehta, K. Spring, S. Kozlov, M.F. Lavin, R.A. Gatti, P. Concannon, and K. Khanna. 2000. ATM-dependent phosphorylation of nibrin in response to radiation exposure. *Nat. Genet.* 25:115–119.
18. Wu, X., V. Ranganathan, D.S. Weisman, W.F. Heine, D.N. Ciccone, T.B. O'Neill, K.E. Crick, K.A. Pierce, W.S. Lane, G. Rathbun, et al. 2000. ATM phosphorylation of Nijmegen breakage syndrome protein is required in a DNA damage response. *Nature.* 405:477–482.
19. Kastan, M.B., and D.S. Lim. 2000. The many substrates and functions of ATM. *Nat. Rev. Mol. Cell Biol.* 1:179–186.
20. Shiloh, Y. 2003. ATM and related protein kinases: safeguarding genome integrity. *Nat. Rev. Cancer.* 3:155–168.
21. Bakkenist, C.J., and M.B. Kastan. 2003. DNA damage activates ATM through intermolecular autophosphorylation and dimer dissociation. *Nature.* 421:499–506.
22. Lee, J.H., and T.T. Paull. 2004. Direct activation of the ATM protein kinase by the Mre11/Rad50/Nbs1 complex. *Science.* 304:93–96.
23. Andegeko, Y., L. Moyal, L. Mittelman, I. Tsarfaty, Y. Shiloh, and G. Rotman. 2001. Nuclear retention of ATM at sites of DNA double strand breaks. *J. Biol. Chem.* 276:38224–38230.
24. Perkins, E.J., A. Nair, D.O. Cowley, T. Van Dyke, Y. Chang, and D.A. Ramsden. 2002. Sensing of intermediates in V(D)J recombination by ATM. *Genes Dev.* 16:159–164.
25. Boultwood, J. 2001. Ataxia telangiectasia gene mutations in leukaemia and lymphoma. *J. Clin. Pathol.* 54:512–516.
26. Taylor, A.M., J.A. Metcalfe, J. Thick, and Y.F. Mak. 1996. Leukemia and lymphoma in ataxia telangiectasia. *Blood.* 87: 423–438.
27. Barlow, C., S. Hirotsune, R. Paylor, M. Liyanage, M. Eckhaus, F. Collins, Y. Shiloh, J.N. Crawley, T. Ried, D. Tagle, and A. Wynshaw-Boris. 1996. Atm-deficient mice: a paradigm of ataxia telangiectasia. *Cell.* 86:159–171.
28. Xu, Y., T. Ashley, E.E. Brainerd, R.T. Bronson, M.S. Meyn, and D. Baltimore. 1996. Targeted disruption of ATM leads to growth retardation, chromosomal fragmentation during meiosis, immune defects, and thymic lymphoma. *Genes Dev.* 10:2411–2422.
29. Xu, Y. 1999. ATM in lymphoid development and tumorigenesis. *Adv. Immunol.* 72:179–189.
30. Liyanage, M., Z. Weaver, C. Barlow, A. Coleman, D.G. Pankratz, S. Anderson, A. Wynshaw-Boris, and T. Ried. 2000. Abnormal rearrangement within the alpha/delta T-cell receptor locus in lymphomas from Atm-deficient mice. *Blood.* 96:1940–1946.
31. Waldmann, T.A., S. Broder, C.K. Goldman, K. Frost, S.J. Korsmeyer, and M.A. Medici. 1983. Disorders of B cells and helper T cells in the pathogenesis of the immunoglobulin deficiency of patients with ataxia telangiectasia. *J. Clin. Invest.* 71:282–295.
32. McFarlin, D.E., W. Strober, and T.A. Waldmann. 1972. Ataxia-telangiectasia. *Medicine (Baltimore).* 51:281–314.
33. Pan, Q., C. Petit-Frere, A. Lahdesmaki, H. Gregorek, K.H. Chrzanowska, and L. Hammarstrom. 2002. Alternative end joining during switch recombination in patients with ataxia-telangiectasia. *Eur. J. Immunol.* 32:1300–1308.
34. Pan-Hammarstrom, Q., S. Dai, Y. Zhao, I.F. van Dijk-Hard, R.A. Gatti, A.L. Borresen-Dale, and L. Hammarstrom. 2003. ATM is not required in somatic hypermutation of VH, but is involved in the introduction of mutations in the switch mu region. *J. Immunol.* 170:3707–3716.
35. Liao, M.J., C. Yin, C. Barlow, A. Wynshaw-Boris, and T. van Dyke. 1999. Atm is dispensable for p53 apoptosis and tumor suppression triggered by cell cycle dysfunction. *Mol. Cell. Biol.* 19:3095–3102.
36. Jumper, M.D., Y. Nishioka, L.S. Davis, P.E. Lipsky, and K. Meek. 1995. Regulation of human B cell function by recombinant CD40 ligand and other TNF-related ligands. *J. Immunol.* 155:2369–2378.
37. Winter, D.B., Q.H. Phung, A. Umar, S.M. Baker, R.E. Tarone, K. Tanaka, R.M. Liskay, T.A. Kunkel, V.A. Bohr, and P.J. Gearhart. 1998. Altered spectra of hypermutation in antibodies from mice deficient for the DNA mismatch repair protein PMS2. *Proc. Natl. Acad. Sci. USA.* 95:6953–6958.
38. Reina-San-Martin, B., S. Difilippantonio, L. Hanitsch, R.F. Masilamani, A. Nussenzweig, and M.C. Nussenzweig. 2003. H2AX is required for recombination between immunoglobulin switch regions but not for intra-switch region recombination or somatic hypermutation. *J. Exp. Med.* 197:1767–1778.
39. Ammann, A.J., W.A. Cain, K. Ishizaka, R. Hong, and R.A. Good. 1969. Immunoglobulin E deficiency in ataxia-telangiectasia. *N. Engl. J. Med.* 281:469–472.
40. Oxelius, V.A., A.I. Berkel, and L.A. Hanson. 1982. IgG2 deficiency in ataxia-telangiectasia. *N. Engl. J. Med.* 306:515–517.
41. Peterson, R.D., M.D. Cooper, and R.A. Good. 1966. Lymphoid tissue abnormalities associated with ataxia-telangiectasia. *Am. J. Med.* 41:342–359.
42. Fiorilli, M., L. Businco, F. Pandolfi, R. Paganelli, G. Russo, and F. Aiuti. 1983. Heterogeneity of immunological abnormalities in ataxia-telangiectasia. *J. Clin. Immunol.* 3:135–141.
43. Snapper, C.M., L.M. Pecanha, A.D. Levine, and J.J. Mond. 1991. IgE class switching is critically dependent upon the nature of the B cell activator, in addition to the presence of IL-4.

J. Immunol. 147:1163–1170.
44. Forni, L., M. Bjorklund, and A. Coutinho. 1988. Membrane expression of IgG but not maturation to secretion requires DNA replication. *J. Mol. Cell. Immunol.* 4:59–70.
45. Chu, C.C., W.E. Paul, and E.E. Max. 1992. Quantitation of immunoglobulin mu-gamma 1 heavy chain switch region recombination by a digestion-circularization polymerase chain reaction method. *Proc. Natl. Acad. Sci. USA.* 89:6978–6982.
46. Morrison, C., E. Sonoda, N. Takao, A. Shinohara, K. Yamamoto, and S. Takeda. 2000. The controlling role of ATM in homologous recombinational repair of DNA damage. *EMBO J.* 19:463–471.
47. Rolink, A., F. Melchers, and J. Andersson. 1996. The SCID but not the RAG-2 gene product is required for S mu-S epsilon heavy chain class switching. *Immunity.* 5:319–330.
48. Manis, J.P., Y. Gu, R. Lansford, E. Sonoda, R. Ferrini, L. Davidson, K. Rajewsky, and F.W. Alt. 1998. Ku70 is required for late B cell development and immunoglobulin heavy chain class switching. *J. Exp. Med.* 187:2081–2089.
49. Casellas, R., A. Nussenzweig, R. Wuerffel, R. Pelanda, A. Reichlin, H. Suh, X.F. Qin, E. Besmer, A. Kenter, K. Rajewsky, and M.C. Nussenzweig. 1998. Ku80 is required for immunoglobulin isotype switching. *EMBO J.* 17:2404–2411.
50. Schubert, R., J. Reichenbach, and S. Zielen. 2002. Deficiencies in CD4+ and CD8+ T cell subsets in ataxia telangiectasia. *Clin. Exp. Immunol.* 129:125–132.
51. Giovannetti, A., F. Mazzetta, E. Caprini, A. Aiuti, M. Marziali, M. Pierdominici, A. Cossarizza, L. Chessa, E. Scala, I. Quinti, et al. 2002. Skewed T-cell receptor repertoire, decreased thymic output, and predominance of terminally differentiated T cells in ataxia telangiectasia. *Blood.* 100:4082–4089.
52. Khanna, K.K., J. Yan, D. Watters, K. Hobson, H. Beamish, K. Spring, Y. Shiloh, R.A. Gatti, and M.F. Lavin. 1997. Defective signaling through the B cell antigen receptor in Epstein-Barr virus-transformed ataxia-telangiectasia cells. *J. Biol. Chem.* 272:9489–9495.
53. Stavnezer-Nordgren, J., and S. Sirlin. 1986. Specificity of immunoglobulin heavy chain switch correlates with activity of germline heavy chain genes prior to switching. *EMBO J.* 5:95–102.
54. Yancopoulos, G.D., R.A. DePinho, K.A. Zimmerman, S.G. Lutzker, N. Rosenberg, and F.W. Alt. 1986. Secondary genomic rearrangement events in pre-B cells: VHDJH replacement by a LINE-1 sequence and directed class switching. *EMBO J.* 5:3259–3266.
55. Arudchandran, A., R.M. Bernstein, and E.E. Max. 2004. Single-stranded DNA breaks adjacent to cytosines occur during Ig gene class switch recombination. *J. Immunol.* 173: 3223–3229.
56. Manis, J.P., D. Dudley, L. Kaylor, and F.W. Alt. 2002. IgH class switch recombination to IgG1 in DNA-PKcs-deficient B cells. *Immunity.* 16:607–617.
57. Manis, J.P., J.C. Morales, Z. Xia, J.L. Kutok, F.W. Alt, and P.B. Carpenter. 2004. 53BP1 links DNA damage-response pathways to immunoglobulin heavy chain class-switch recombination. *Nat. Immunol.* 5:481–487.
58. Petersen, S., R. Casellas, B. Reina-San-Martin, H.T. Chen, M.J. Difilippantonio, P.C. Wilson, L. Hanitsch, A. Celeste, M. Muramatsu, D.R. Pilch, et al. 2001. AID is required to initiate Nbs1/gamma-H2AX focus formation and mutations at sites of class switching. *Nature.* 414:660–665.
59. Celeste, A., S. Petersen, P.J. Romanienko, O. Fernandez-Capetillo, H.T. Chen, O.A. Sedelnikova, B. Reina-San-Martin, V. Coppola, E. Meffre, M.J. Difilippantonio, et al. 2002. Genomic instability in mice lacking histone H2AX. *Science.* 296:922–927.
60. Mochan, T.A., M. Venere, R.A. DiTullio Jr., and T.D. Halazonetis. 2003. 53BP1 and NFBD1/MDC1-Nbs1 function in parallel interacting pathways activating ataxia-telangiectasia mutated (ATM) in response to DNA damage. *Cancer Res.* 63:8586–8591.
61. Xia, Z., J.C. Morales, W.G. Dunphy, and P.B. Carpenter. 2001. Negative cell cycle regulation and DNA damage-inducible phosphorylation of the BRCT protein 53BP1. *J. Biol. Chem.* 276:2708–2718.
62. Schultz, L.B., N.H. Chehab, A. Malikzay, and T.D. Halazonetis. 2000. p53 binding protein 1 (53BP1) is an early participant in the cellular response to DNA double-strand breaks. *J. Cell Biol.* 151:1381–1390.
63. Severinson, E., S. Bergstedt-Lindqvist, W. van der Loo, and C. Fernandez. 1982. Characterization of the IgG response induced by polyclonal B cell activators. *Immunol. Rev.* 67: 73–85.
64. Kenter, A.L., and J.V. Watson. 1987. Cell cycle kinetics model of LPS-stimulated spleen cells correlates switch region rearrangements with S phase. *J. Immunol. Methods.* 97:111–117.
65. van der Loo, W., E.S. Gronowicz, S. Strober, and L.A. Herzenberg. 1979. Cell differentiation in the presence of cytochalasin B: studies on the "switch" to IgG secretion after polyclonal B cell activation. *J. Immunol.* 122:1203–1208.